Innovation, Sciences et Développement économique Canada
Office de la Propriété Intellectuelle du Canada

Innovation, Science and Economic Development Canada
Canadian Intellectual Property Office

CA 2893408 C 2018/05/29

(11)(21) **2 893 408**

(12) **BREVET CANADIEN**
CANADIAN PATENT

(13) **C**

(86) Date de dépôt PCT/PCT Filing Date: 2013/12/05
(87) Date publication PCT/PCT Publication Date: 2014/06/12
(45) Date de délivrance/Issue Date: 2018/05/29
(85) Entrée phase nationale/National Entry: 2015/05/28
(86) N° demande PCT/PCT Application No.: EP 2013/075647
(87) N° publication PCT/PCT Publication No.: 2014/086919
(30) Priorités/Priorities: 2012/12/07 (DE10 2012 023 895.9); 2013/02/21 (DE10 2013 202 881.4)

(51) Cl.Int./Int.Cl. *F03D 1/06* (2006.01)
(72) Inventeurs/Inventors:
ALTMIKUS, ANDREE, DE;
KAMRUZZAMAN, MOHAMMAD, DE
(73) Propriétaire/Owner:
WOBBEN PROPERTIES GMBH, DE
(74) Agent: OYEN WIGGS GREEN & MUTALA LLP

(54) Titre : BORD DE FUITE DE PALE DE ROTOR
(54) Title: ROTOR BLADE TRAILING EDGE

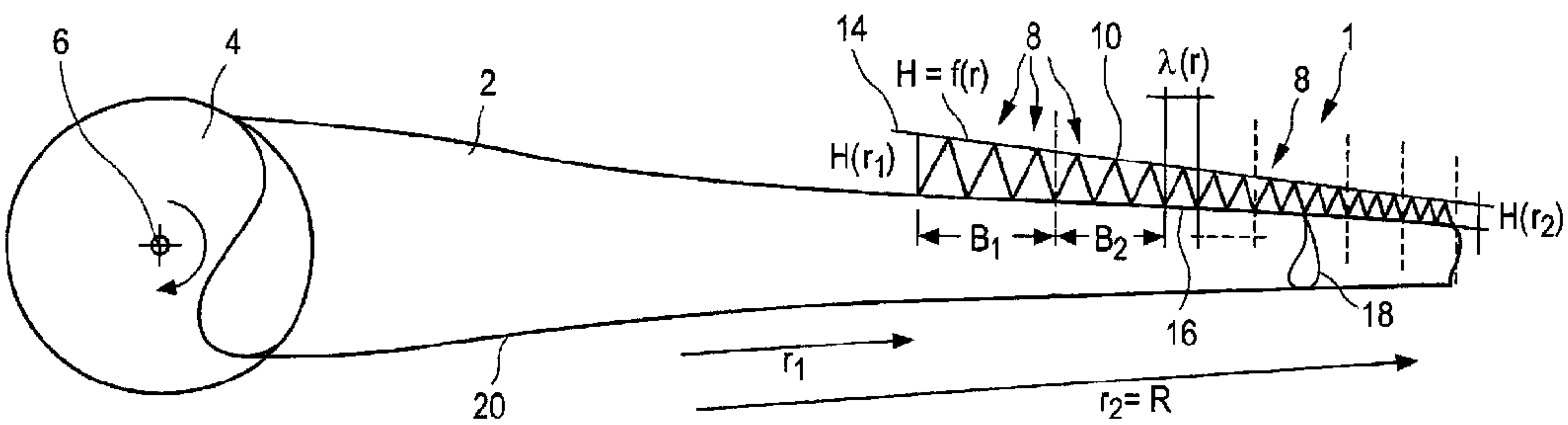

(57) Abrégé/Abstract:
A method for calculating a trailing edge that is to be produced for a rotor blade of an aerodynamic rotor of a wind power installation, wherein the rotor blade has radial positions with respect to the rotor, the rotor blade has a local blade profile that is a function of the radial positions with respect to the rotor and the trailing edge has a jagged profile having a plurality of spikes, wherein each spike has a spike height and a spike width, and the spike height and/or the spike width is calculated as a function of the radial position thereof and/or as a function of the local blade profile of the radial position thereof.

Abstract

A method for calculating a trailing edge that is to be produced for a rotor blade of an aerodynamic rotor of a wind power installation, wherein the rotor blade has radial positions with respect to the rotor, the rotor blade has a local blade profile that is a function of the radial positions with respect to the rotor and the trailing edge has a jagged profile having a plurality of spikes, wherein each spike has a spike height and a spike width, and the spike height and/or the spike width is calculated as a function of the radial position thereof and/or as a function of the local blade profile of the radial position thereof.

Fig. 2

Rotor blade trailing edge

The invention relates to the design of the trailing edge of a rotor blade of a wind power installation, or to a method for calculating a trailing edge to be produced respectively. Furthermore, the present invention relates to a trailing edge for a rotor blade and the invention relates to a rotor blade having a trailing edge. Moreover, the present invention relates to a wind power installation having at least one rotor blade having a trailing edge.

Wind power installations are generally known and Figure 1 shows a known wind power installation. The design of the rotor blade or of the rotor blades respectively is an aspect that is important to the efficiency of the wind power installation. In addition to the basic profile of the rotor blade, the rotor blade trailing edge also has an influence on the behavior of the rotor blade.

In this context, saw tooth-shaped trailing edges or trailing edges having a jagged profile having a plurality of spikes respectively have also been proposed. However, providing such a saw tooth-shaped trailing edge can be expensive and there is a risk that providing a jagged trailing edge or saw tooth-shaped trailing edge respectively will create an expense that is not proportional to the effect.

From EP 0 652 367 A1, it is known that the trailing edge should be saw-tooth shaped in the longitudinal direction of the main spar of the rotor blade, in order to reduce the noise level.

From EP 1 314 885 B1, it is known that the trailing edge should be saw-tooth shaped in the longitudinal direction of the main spar of the rotor blade and, at the same time, flexible, in order to increase the torque that the rotor blade exerts on the generator.

The object of the present invention is to address at least one of the problems mentioned above. In particular, a solution should be proposed that further increases the effectiveness of a rotor blade of a wind power installation.

The object of the invention is, in particular, to further increase the effectiveness of a rotor blade without increasing the noise effects. An alternative solution should at least be provided.

For this purpose, a rotor blade is proposed, the trailing edge of which is designed in a saw-tooth shape in the longitudinal direction of the main spar of the rotor blade, wherein the distance and/or length are functionally dependent on the local flow conditions at the blade profile and the thickness of the turbulent boundary layer that develop therefrom, or on the coherence length scales of the bales of turbulence with the pressure fluctuations forming therein respectively. The length of the individual teeth should preferably change from tooth to tooth.

Consequently, a saw tooth-shaped trailing edge is proposed, which accordingly has a plurality of spikes or teeth, which terms are used synonymously here, which taper to a point away from the rotor blade, essentially towards the rear, namely the side facing away from the intended rotational movement of the rotor. Accordingly, the spaces between respectively two spikes or teeth taper to a point in the direction of the rotor blade. Such spikes have a height, namely the distance from the base line, at which the spaces that taper to a point end, to the crown line, at which the spikes that taper to a point end, as the crown line, which connects the spike tips. This base line and this crown line may be curved lines and may have a variable distance from one another along the length of the blade.

The length of the individual teeth can synonymously be referred to as the height of the teeth or the height of the spikes respectively, thus as the spike height.

According to the invention, a method is proposed for calculating a trailing edge to be produced as described below. Thus, a trailing edge is proposed which is to be produced for a rotor blade of an aerodynamic rotor of a wind power installation. The rotor blade has radial positions with respect to this rotor, in which the rotor blade is to be used or is used respectively. A radial position of the trailing edge and of the rotor blade thus always refers to this rotor, thus to the distance from the rotation axis of the rotor. This approach is also used as a basis for a rotor blade that is initially not yet installed. A rotor blade of a wind power installation is essentially adapted to a specific wind power installation, in particular to the rotor having this rotor blade and usually two additional rotor blades.

For that purpose, the rotor blade has a local blade profile at each radial position. In other words, each blade profile has its own blade profile depending on its radial position.

The trailing edge has a jagged profile having a plurality of spikes, which can also be referred to as saw tooth-shaped. Here, the individual spikes are essentially mirror symmetrical, and thus have two oblique, approximately identical flanks. In particular, these teeth regularly do not have a vertical and an oblique flank, but rather, two oblique flanks.

Each spike has a spike height and a spike width. The spike height is the distance between a base line and a crown line already described above. The spike width is the distance of the respective end of the two spaces that taper to a point, which spaces delimit the spike. As a first approximation, the width of the spike is the distance from the spike tip thereof to the spike tip of an adjacent spike. These spikes of a proposed spike-shaped trailing edge preferably differ from one another, however this difference is comparatively small for immediately adjacent spikes.

It is now proposed that the spike height and, in addition or alternatively, the spike width, be calculated as a function of the radial position thereof. Thus there is a separate calculation for each spike, depending on the radial position thereof. As a result, a trailing edge is hereby created having many spikes, which were calculated individually and accordingly may have individual sizes, which in particular change quasi continuously across the length of the rotor blade with increased or decreased radial position respectively.

The spike height and, in addition or alternatively, the spike width, is preferably calculated as a function of the local blade profile of the radial position thereof. The blade profile of the radial position of a spike, or in other words the profile of the blade profile in this radial position, is thus considered.

According to one embodiment, it is proposed that the spike height be greater than the spike width and that the spike width be calculated from the spike height. The ratio of the spike height to the spike width falls in the range of 0.5 to 10, in particular 3 to 5 for this calculation. Preferably it has a value of approximately 4, in particular a value of 2. The spike width λ can thus be calculated from the spike height H according to the formula:

$$\lambda = H / k_n \text{ where } k_N = [0{,}5 \ldots 10], \text{ in particular } \quad k_N = 2$$

The spike is thus comparatively narrow and, in particular, tapers to an acute angle. A ratio in this range has proven to be particularly advantageous in minimizing noise, at least for those individually calculated spikes. Especially in the case that the spike height is in a fixed ratio to the spike width, the result is the same whether the spike height is calculated first and then the spike width calculated therefrom, or whether the spike width is first calculated and then the spike height calculated therefrom.

The spikes preferably have different spike widths and/or different spike heights and thereby differ from one another individually.

The calculation is preferably set up in such a way that, in the case of trailing edges for low-wind locations, the spike height of the spikes decreases with reference to the profile depth as the radius of the radial position of the spikes thereof increases, while in the case of trailing edges for strong-wind locations, the spike height of the spikes increases with reference to the profile depth as the radius of the radial position of the spikes thereof increases. This is due to the wind class-specific blade design.

In the wind energy industry, it is common to classify sites according to wind classes. As a rule, stronger wind can be expected in strong-wind locations, which exist in particular in the coastal regions or off-shore locations. The wind power installation, in particular the rotor blades, are designed accordingly, namely so that they can stand up to strong winds, and the wind power installation can thereby also be operated such that they are able to capture less energy from the wind than with a wind power installation for low-wind locations.

Accordingly, wind power installations for low-wind locations, which predominate in particular at inland locations, are designed in such a way that they do not need to be able to stand up to strong winds, or at least not during operation, but must be regulated at least for wind forces for which a wind power installation for a strong-wind location would not yet require regulation. In turn, a wind power installation of this kind for low-wind locations can capture more energy in in weak wind. A person skilled in the art is familiar with classifications of this kind and, in some cases, might distinguish even more sub-classifications.

According to one embodiment, it is thereby proposed that the calculation be set up in such a way that spike heights decrease with reference to the profile depth for rotor blades of wind power installations for low-wind locations as the radius increases. For example, in the case of a trailing edge for a low-wind location, the slope of the change in spike height H

$$\frac{\partial(H/c)}{\partial(r/R)} = [-15\ldots-25], \text{in particular} = -20$$

for a standardized radius can be from 0.6 to 0.8 with reference to the radius. Thus there is a decrease in the spike height and here, the spike height H in relation to the profile depth c is considered in the numerator, and the Radius r in relation to the maximum radius of the rotor blade R is considered in the numerator. The spike height in reference to the profile depth preferably has a constant progression between r/R = 0.75 and r/R = 0.9, and first drops off again to the maximum radius R at r/R=0.9. This is also illustrated in the drawings as discussed below.

For a trailing edge for a wind power installation of the same power class, but for a strong-wind location, the corresponding ratio may be positive and may have a value of +20 because the spike height, which can also be referred to as the spike depth, increases. The spike height reaches a maximum at 0.85r/R and then undergoes a strict monotonic decrease to the blade tip.

Such a calculation of the trailing edge based on the wind class accommodates various problems that arise according to the wind class.

The spike height and/or the spike width is preferably calculated as a function of the local radius thereof by means of a polynomial relationship, preferably a fourth to eighth degree polynomial relationship, in particular fifth or sixth degree, in particular sixth degree for low-wind locations and fifth degree for strong-wind locations. The characteristic progression of spike heights may differ fundamentally between low-wind locations and strong-wind locations. This can be accounted for by using polynomials of different grades for low-wind locations and strong-wind locations.

The calculation is preferably dependent on one or more anticipated noise spectra. In addition or alternatively, the calculation depends on one more operating points. It is thus proposed that the behavior of the wind power installation be concretely taken into account for at least one operating point. In this respect, an operating point of this kind is an idealized, stationary operating point, which in particular is defined by a wind speed, a rotational speed of the rotor of the wind power installation and/or power generated by the wind power installation. The blade angle of the rotor blade to the wind can also influence this operating point.

An anticipated noise spectrum is now determined for at least one such operating point, namely a noise level or a sound level or a noise threshold as a function of the frequency of this noise. As a rule, this results in a frequency-dependent progression having a maximum value. This spectrum is included in the calculation. In particular, the frequency of this spectrum at which this maximum value is reached is taken into account. This frequency can be referred to as the peak frequency or maximum frequency, and in German is also frequently referred to as "peak frequency." If the operating point is now modified, a new spectrum and therefore a new peak frequency arises. Thus frequency spectra and therefore peak frequency values may be recorded for each individual spike at a plurality of operating points. In order to calculate the relevant spikes, a peak frequency is used for that purpose, and one peak frequency can be selected from among the plurality of peak frequencies that were determined. The peak frequency that is used can also be an averaged value from the plurality of peak frequencies that were recorded. The recording and evaluation of frequency spectra is also explained as an example in the drawings as described below.

In order to record these frequency spectra and ultimately the respective peak frequencies, it is possible to conduct tests in a wind tunnel. Likewise, there are simulation methods that can be used to determine spectra and peak frequencies of this kind.

The set operating point and, if applicable, also the modification of the operating points are based in particular on real operating points. Here, many control processes of a wind power installation work in such a way that an operating point is essentially assigned to each wind speed. This can at least be assumed, by way of simplification, when effects such as different levels of turbulence, very strong wind, or very strongly increasing or decreasing wind are omitted from considerations by way of simplification. Thus two or three or four specific operating points are preferably selected from the range of wind speeds, which should cover the wind power installation in question.

The effective flow velocity that is assigned to the respective operating point is preferably included in the calculation of the respective spike, in particular spike height. The effective or local flow velocity V_{eff} is the speed that arises from the perspective of the rotor blade at the appropriate position, thus at the appropriate radial position, from the vectorial addition of the wind speed and the movement velocity of the rotor blade at this position.

The calculation is preferably carried out depending on the respective local profile. Thus the profile is included in the calculation or may also be included in measurements taken during tests in the wind tunnel. The local flow velocity may also depend upon the profile and/or upon the position of the rotor blade and therefore upon the position of the profile.

The calculation of the spike height H of a prescribed radial position is preferably carried out based on the associated flow velocity V_{eff}, the associated peak frequency f_{peak} of the noise spectrum of an operating point, and depending on a predetermined factor k, which can be determined empirically and which, for example, may also exist as an empirical value. On this basis, the spike height H can then be calculated according to the formula:

$$H = k \cdot \frac{V_{eff}}{f_{peak}}.$$

This calculation is based on the following consideration.

The spike height H is calculated from the coherence length scale $\Lambda_{p,3}$ or Λ_{p3} of the turbulent pressure fluctuation within the meaning and with the help of the Corcos model [3] respectively, and by using a constant factor c_2 according to the following equation:

$$H = c_2 \cdot \Lambda_{p3}.$$

The factor c_2 can be determined empirically, for example from test measurements. Empirical values may also be used for c_2. Λ_{p3} is a function of the radius of the rotor, in which the rotor blade is used. The coherence length scale Λ_{p3} can be calculated from the convection velocity U_c and the peak frequency f_{peak}, which is also known in German-speaking countries as the peak frequency, according to the following calculation:

$$\Lambda_{p3} = \frac{U_c}{\left(2 \cdot \pi \cdot f_{peak}\right)}.$$

The convection velocity U_c is calculated from the effective or from the local flow velocity V_{eff} respectively at the blade profile by means of the constant c_1, which can be determined empirically through testing or simulations and in particular has the value 0.7 (c_1=0.7), according to the equation:

$$U_c = c_1 \cdot V_{eff}$$

The effective or local flow velocity V_{eff} respectively is calculated with the help of a blade element momentum method, which is also known by the acronym BEM (from the English term, "Blade Element Momentum method").

The pitch angle of the rotor blade, the rotational speed of the rotor, the wind speed as well as the concrete radius and the blade profile of the blade profile at the radial position and the local torsional angle thereof on the rotor blade are included in this calculation, for which the flow velocity V_{eff} and therefore the spike height H are to be calculated. The calculation is thus carried out for a specific operating point.

The peak frequency f_{peak} is the frequency at which the greatest noise level occurs or is to be anticipated, respectively, for the operating point being examined and the radial position on the rotor blade being examined, in reference to the rotor. Thus, it is the frequency at which a trailing edge noise spectrum or trailing edge sound spectrum respectively is at its maximum.

The peak frequency f_{peak} can be determined empirically, for example by conducting dedicated experiments in the wind tunnel, for example with dynamic pressure sensors at the trailing edge of the wind tunnel specimen, or can be calculated using a numerical aeroacoustic simulation for the local Reynolds number Re. The local Reynolds number is obtained from the local angle of incidence α, the local flow velocity and the local profile depth, and can also be obtained as a result using the specified BEM. Furthermore, the two-dimensional profile geometry of the local blade profile is also included.

The spike height H is thus calculated from the following ratio of the flow velocity V_{eff} to the peak frequency f_{peak} of the noise spectrum according to the formula:

$$H = \frac{c_2 \cdot c_1 \cdot V_{eff}}{(2 \cdot \pi \cdot f_{peak})} = \frac{k \cdot V_{eff}}{f_{peak}}$$

with $k = \frac{c_2 \cdot c_1}{(2 \cdot \pi)}$.

Here, V_{eff} and f_{peak} are dependent on the blade angle of the rotor blade, the rotational speed of the rotors, the wind speed as well as the concrete radius and the blade profile of the blade profile of the radial position on the rotor blade, for which the spike height H is to be determined.

What is moreover proposed in accordance with the invention is a trailing edge as described below. Such a trailing edge is distinguished by a jagged profile, which has spikes having a spike height and spike width, wherein the spike height and/or the spike width is dependent on the radial position thereof and/or on the local blade profile of the radial position thereof.

Thus the relationships, explanations and advantages arise pursuant to at least one embodiment of the described method for calculating a trailing edge to be produced.

A trailing edge is preferably proposed that is calculated using a method pursuant to one of the embodiments described above.

A trailing edge for a rotor blade can also be referred to as a rotor blade trailing edge.

The calculation of the spike height H is preferably carried out for a predetermined radial position from the corresponding coherence length scale Λ_{p3}, taking into account a constant factor c_2 with the formula:

$$H = c_2 \cdot \Lambda_{p3}.$$

Consequently, for the spike of the corresponding radius, the coherence length scale for the same radius is included in the calculation. The coherence length scale Λ_{p3} is a function that is dependent on the radius of the rotor and, accordingly, a function that is dependent on the radius arises for the spike heights of the trailing edge. The amplitude of this function can be proportionally increased or decreased by means of the constant factor c_2, whereby the basic progression of this function is not changed, however. A range can be spanned by a curve having a very small c_2 and an additional curve having a very large c_2, in which an advantageous function for the spike heights can be selected.

A rotor blade for a wind power installation having a trailing edge pursuant to at least one described embodiment is preferably proposed.

In addition, a wind power installation having one, and in particular, three such rotor blades is preferably proposed.

The invention is described in greater detail below, using embodiments as examples with reference to the accompanying figures.

Figure 1 shows the schematic perspective view of a wind turbine.

Figure 2 shows a schematic view of a rotor blade having a trailing edge with a jagged profile having a plurality of spikes.

Figure 3 shows a schematic view of a section of a rotor blade in a top view having a schematic contour for a strong wind turbine and having a dashed line showing a deviating contour for a low wind turbine.

Figure 4 shows a schematic view of a blade profile of a rotor blade having a schematically illustrated turbulence region.

Figure 5 shows a schematic view of the progression of the spike height H pursuant to at least one embodiment as a function of the radius.

Figure 6 shows frequency spectra at selected sample radius positions of an embodiment.

Figure 7 shows local, aerodynamic parameters that are the basis for a BEM calculation or that are calculated therewith respectively.

Figure 8 shows the peak frequency for an embodiment as a function of the radius.

Figure 9 shows a diagram of different possible progressions of the spike height H as a function of the radius for a strong wind turbine.

Figure 10 shows a diagram of different possible progressions of the spike height H as a function of the radius for a low wind turbine.

Figure 11 shows a diagram of the progression of spike heights, which are scaled for the respective local profile depth over the dimensionless radius for strong wind and low wind design.

Figures 12a and 12b show a trailing edge for a strong wind turbine.

Figures 13a and 13b show a trailing edge for a low wind turbine.

The explanation of the invention based on examples and with reference to the figures is essentially schematic and the elements, which are explained in the respective figure, may be exaggerated for the sake of illustration, while other elements may be simplified. Thus, for example, Figure 1 schematically illustrates a wind power installation in such a way that the provided, spike-shaped trailing edge is not visible.

Figure 1 shows a wind power installation 100 having a tower 102 and a nacelle 104. A rotor 106 with three rotor blades 108 and a spinner 110 is arranged on the nacelle 104.

The rotor 106 is set in operation by the wind in a rotational movement and thereby drives a generator in the nacelle 104.

Figure 2 shows a schematic view of a rotor blade 2 having rotor blade trailing edge 1, which, for the sake of simplicity, is also referred to as a trailing edge. The rotor blade is attached to a hub 4 as intended, which is indicated here only schematically, in order to rotate around a rotation axis 6 of the hub 4.

The trailing edge 1 has a jagged profile having a plurality of spikes 8, which are arranged adjacently along the rotor blade 2. This trailing edge 1 having the spikes 8 is arranged here only on the outer half of the rotor blade 2. Each spike has a radial position, which relates to the rotation axis 6. The first spike 8 starts at the radius r_1 and the last spike 8 ends at the radius r_2, which at the same time corresponds to the total radius R of the rotor blade 2 in reference to the rotation axis 6.

Each spike 8 has a height H, which depends on the respective radius r. The height H of the spikes 8 is thus a function of the radius r:

$$H = f(r).$$

Accordingly, the height of the spike 8 at the radius r_1 is the height $H(r_1)$, and the height H of the last spike is the height $H(r_2)$. The width of each spike 8 is indicated in Figure 2 with the Greek letter λ, which likewise depends on the respective radius r and therefore is represented as $\lambda(r)$.

Each spike 8 has a spike tip 10 and there is a recess having a recess apex 12 between each pair of spikes 8. A line connecting the spike tips 10 can be referred to as a crown line 14 and is shown as a dashed line in Figure 2. A base line or baseline 16 connects the apexes of the recesses 12 and may, as is the case in the illustrated example in Figure 2, illustrate a rear line of the rotor blade 2, which would form a trailing edge of the rotor blade 2 if the jagged trailing edge 1 that is shown were not present.

The distance between the crown line 14 and the base line 16 is not constant and, for the respective radius r, indicates the height H of the spike 8 arranged thereon. Accordingly, the height H of the spike 8 changes depending on the local radius r of the rotor blade 2. For layout or attachment, a plurality of spikes 8 can be grouped, as the shown widths B_1 and B_2 indicate. The calculation of the spikes 8, in particular the height H of the spikes 8, depends on the profile of the respective blade profile, and such a blade profile 18 of this kind is presented for the purpose of illustration.

The width λ or $\lambda(r)$ respectively can also change with the radius r and, in particular, is in a fixed ratio to the height H of the respective spike 8. This ratio is preferably 2, so that the height H of a spike 8 is thus twice as large as the width λ of the same spike. If, according to other embodiments, the ratio of the height H to the width λ is significantly greater than 2, it can be especially useful for manufacturing considerations to form the current spikes 8 so that they are rectangular or approximately rectangular, so that a comb structure is created for the trailing edge, or the trailing edge has crenellations instead of spikes.

Figure 3 shows a rotor blade 2, which may differ from the rotor blade 2 in Figure 2, however. This rotor blade 2 in Figure 3 has a leading edge 20 and a trailing edge 1, the spike-like progression thereof not being shown here for the sake of clarity. This rotor blade 2 having the leading edge 20 and the trailing edge 1 illustrates a basic form of a rotor blade of a strong wind turbine. As a comparison thereto, a trailing edge 1' is shown as a dashed line, which belongs to a rotor blade 2 of a low wind turbine, thus to a wind power installation for low-wind locations. For purposes of illustration, the rotation axis 6 is shown, in order to illustrate the rotational direction of the blade 2 and to render the side of the rotor blade 2 facing the hub, thus facing the rotation axis 6.

In any case, it can be seen in the illustration in Figure 3 that a rotor blade of a low wind turbine has a slimmer design, in particular in the outer region, than a rotor blade of a strong wind turbine. Figure 3 is only intended to illustrate this and it must be pointed out that it can be expected that a rotor blade of a low wind turbine will tend to be longer, thus having a larger radius than a rotor blade of a low wind turbine of the same power class.

Figure 4 illustrates flow conditions on a rotor blade 2 of a wind power installation. Figure 4 thereby shows a blade profile, which may be the blade profile 18 pursuant to Figure 2, for example. Inflowing wind 22, which is simply shown as a line here, splits at the rotor blade 2 in the region of the leading edge 20 thereof and initially continues in a laminar flow. In particular, there is a laminar flow of wind flows on the pressure side 24 up to the vicinity of the trailing edge 1. A boundary layer in which turbulence or eddies may form arises at the suction side 26. The thickness of the boundary layer increases with increased proximity to the trailing edge. The thickness is shown here as δ_1. This increase in the thickness of the boundary layer δ_1 towards the trailing edge 1 leads to correspondingly greater turbulence or eddies arising in the region of the trailing edge 1. In particular, so-called bales of turbulence are encountered in that region of the trailing edge 1. These bales of turbulence are at least partially disrupted or their formation is prevented respectively by the proposed spike-shaped trailing edge. For this purpose, the inclination of the flanks of the spikes 8 (pursuant to Figure 2) should be adjusted as much as possible to these bales of turbulence. The size of the spikes 8 or the space between these should also be adjusted as much as possible to these bales of turbulence. Accordingly, it has been found that the spikes and the space between these cannot be too large or too small. If they are large, such bales of turbulence may linger between two spikes. If the spikes are too small, they will have very little influence on the bales of turbulence. It has thereby been found that the size and manner of the bales of turbulence may depend on the radius at which they occur. The spikes thereby adapt to these radius-dependent bales of turbulence.

Figure 5 shows a sample progression of the height H of spikes 8 of a trailing edge 1 as a function of the radius r. The progression shown is that of a rotor blade of a strong wind turbine. The height H thereby initially increases as the radius r increases, and then decreases again as the radius r continues to increase. The middle curve H_1 shows this progression. In addition, a curve H_2 is shown, which shows a very low, possible progression of the height H, and accordingly a curve H_3 is shown, which correspondingly shows a very large value progression of the height H. These curves H_2 and H_3 may form limiting curves, within which a curve H_1 is preferably selected.

Figure 6 shows four frequency spectra: SPC_1, SPC_2, SPC_3 and SPC_4. These are noise spectra or sound spectra for an installation operating point of the underlying wind power installation at four selected sample radius positions. These four frequency spectra SPC_1, SPC_2, SPC_3 and SPC_4 were recorded at the radius positions r_1=0.39, r_2=0.606, r_3=0.779 or r_4=0.989 respectively. For this purpose, the peak frequencies f_{peak1}, f_{peak2}, f_{peak3} and f_{peak4} were selected accordingly. Each of these noise spectra has a maximum point and the corresponding frequencies are used further as peak frequencies f_{peak} as described. Such a result arises when the noise spectra are recorded at different radial positions of the rotor blade at an operating point of the wind power installation. A radius-dependent function of the maximum values of the peak frequencies and/or a radius-dependent function of the resulting, calculated spike heights H(r) can be determined therefrom.

Figure 7 shows local, aerodynamic parameters for a sample blade profile 18 of a rotor blade 2, which is rotating at the rotational speed Ω along the rotor plane 28, which parameters are needed for a BEM calculation or which are calculated therewith respectively. A vector is drawn for the rotational speed of the rotor Ω, which is opposite to the actual direction of the rotational speed, in order to indicate an associated, calculated wind opposing the movement. The vectorial addition of this calculated wind with the wind or the wind speed V_W thus leads to an effective flow velocity V_{eff}.

Figure 7 thereby illustrates the rotational speed of the rotor Ω, the effective blade angle α, the local installation angle β, which comprises the pitch angle and the torsion of the rotor blade, and the angle of incidence π. In addition, the local profile depth c of the blade profile 18 shown is also plotted. Further, relevant variables are explained in the following table.

Ω *[m/s]*	rotational speed
α *[°]*	effective blade angle
β *[°]*	local installation angle = local torsional angle plus blade pitch angle
λ *[m] or [mm]*	spike width
$\Lambda_{p,3}$ *[m] or [mm]*	span width coherence length of the turbulent pressure fluctuation as a function of the peak frequency f_{peak}
φ *[°]*	inflow angle
V_{eff} *[m/s]*	effective flow velocity
V_W *[m/s]*	wind speed
a'	tangential induction factor
a	axial induction factor
c_l	lift coefficient
c_n	normal force coefficient
c_d	resistance coefficient
c_t	tangential force coefficient
c *[m]*	profile depth
c1	constant =0.7
c2	constant =4…12

dB (-)	decibels (unweighted)
fc[Hz]	mid-range frequency in the third-octave band
fpeak [Hz]	frequency at which the projected sound pressure level engages. Sound Pressure Level (SPL) at its maximum value
h [m] or [mm]	half spike height
H [m] or [mm]	spike height H=2h
Lp,ss [dB(-)]	sound pressure level of the profile suction side
MAX Lambda p,3 [mm]	$\Lambda_{p,3}$coherence length in reference to the maximum of the sound pressure level Lp,ss and of the peak frequency fpeak
r [m]	local radius position on the blade
R [m]	rotor radius
$U_c = 0.7\, V_{eff}$ *[m/s]*	convection velocity eng. convective velocity

The use in connection with a BEM calculation can be found in reference [1].

Now the coherence length scale in particular can also be calculated.

The radius/span width coherence length scale of the turbulent pressure fluctuations was calculated using the Corcos model [3] according to the following equation,

$$\Lambda_{p3} = \frac{U_c}{2 \cdot \pi \cdot f_{peak}}$$

wherein

$$U_c = c_1 \cdot V_{eff}$$

c_1 is a constant having a value of 0.7. U_c is known as convection velocity. The effective or local flow velocity V_{eff} on the blade profile of the radius/span width position r is determined by a calculation using a blade element momentum method (BEM), see Figure 7. The BEM also provides all other needed local flow parameters such as the effective blade angle α , Reynolds (Re) and Mach (Ma) numbers. The parameter f_{peak} is the frequency at which the trailing edge noise spectrum of the boundary layer reaches its maximum. This parameter can either be determined by means of dedicated wind tunnel experiments on the profile, in which the frequency spectrum of the wall pressure fluctuations of the turbulent boundary layer at a point in the immediate vicinity of the trailing edge of the profile is measured, or can be numerically determined using any theoretical noise prediction model.

The noise spectrum and the peak frequency f_{peak} can be determined empirically, for example by conducting dedicated experiments in the wind tunnel, for example with dynamic pressure sensors at the trailing edge of the wind tunnel specimen, or can be calculated using a numerical aeroacoustic simulation for the local Reynolds number Re. The local Reynolds number is obtained from the local angle of incidence α, the local flow velocity and the local profile depth, and can also be obtained as a result using the specified BEM. Furthermore, the two-dimensional profile geometry of the local blade profile is also included.

Λ_{p3} is determined for each profile along the blade span width through the use of the process described above.

The following formulas were used for the definition of the local geometric dimension of the trailing edge spikes:

spike height H as a function of the dimensionless radius

$$H\left(\frac{r}{R}\right) = c_2.\Lambda_{p3}\left(\frac{r}{R}\right)$$

And spike distance

$$\lambda = \frac{H}{2}$$

Wherein $c_2 = c_{onst}$ is an empirical constant in the range of values from 4 to 15. In a preferred embodiment, $c_2 = 8$.

Figure 8 shows a diagram, which illustrates the peak frequency f_{peak} as a function of the radius for an operating point. The peak frequencies f_{peak1} to f_{peak4} correspond to those in in Figure 6 and were obtained as described in Figure 6. In the illustration, a dimensionless illustration was selected for the radius, namely the radius r standardized to the maximum radius R. By way of illustration, many recorded peak frequencies that are a function of the radius r have been plotted and each connected by a line. The illustration shows that the peak frequencies are also higher as the radius increases. Consequently, it can be seen in this illustration that the frequency of the maximum noise or of the maximum sound respectively shifts to higher values as the radius r increases. This can be explained by the fact that bales of turbulence, which can also referred to as turbulence eddies, become smaller as the radius increases.

Figure 9 shows the spike height H as a function of the radius r standardized to the maximized radius R. In this diagram, as in the diagram in Figure 10, only the region of the outer third of the rotor blade being examined is shown. There are 11 discrete values H_r shown in the diagram as a function of the standardized radius, each depicted as a small square. These values were recorded independently by determining a single peak frequency for each respective radius. These discrete spike heights H_r all pertain to the same operating point. A functional correlation is now determined for these discrete values H_r, which is illustrated as curve H_8. This curve H_8 represents a polynomial approximation of these discretely recorded values H_r. Such an approach by means of polynomials can be carried out, for example, by minimizing the standard deviations or the sum of the squares of the deviations. In principle, other approaches may be used such as, for example, a polynomial of a higher or lower degree. This approximated progression H_8 can also be specified as $H = c_2 \cdot \Lambda_{p3}$, wherein here, c_2 has the value 8 ($c_2 = 8$). This radius-dependent function H_8 thus determined thereby indicates progression of the height of the spikes as a function of the radius for an operating point. For other operating points, there are other progressions of the spike height H, which can be expressed by another value for c_2.

Accordingly, the progressions H_4 and H_{10} show corresponding progressions of the spike height H for other operating points, wherein the operating point is equal to the respective curve H_4 or H_{10} respectively for each of the radii shown. It has been found that the inclusion of the discrete H_r value for other operating points is not necessary and modifying the constant c_2 is sufficient in order to represent the progressions of the spike heights H as a function of the radius for other operating points of this kind with good accuracy.

Figure 9 shows the correlations for a strong wind turbine having a design tip speed ratio of 7, namely for a wind power installation by Enercon having the model number E82. Figure 10 shows progressions that are very similar to Figure 9, but for a low wind turbine, namely an E92-1 model installation from Enercon. In this case as well, height progressions H for different operating points are shown, and for improved clarity, the same designations are used as in Figure 9. Thus, a function H_8 exists for an operating point, which approximates multiple discretely recorded values H_r by means of a fifth degree polynomial. The progression H_4 or H_{10} respectively arises for other operating points. The progressions H_8, H_4 and H_{10} are based on the functional correlation $H = c_2 \cdot \Lambda_{p3}$ with $c_2 = 8$, $c_2 = 4$ or $c_2 = 10$ respectively.

In order to obtain a continuous progression along the span width, $\Lambda_{p3}\left(\frac{r}{R}\right)$ was thus calculated at various discrete span width positions and used in the definition of a polynomial of the sixth order by means of an optimal curve fitting. In so doing, the number of polynomial members, namely $\left(\frac{r}{R}\right)^0$ to $\left(\frac{r}{R}\right)^5$, was used to designate the order and thus this designates a fifth degree polynomial.

In the case of the example pursuant to Figure 9, the resulting fifth degree polynomial for the spike height H as a function of the dimensionless blade radius is:

$$H\left(\frac{r}{R}\right) = c_2 \cdot \Lambda_{p3} = c_2 \cdot \left[66808\left(\frac{r}{R}\right)^5 - 281611\left(\frac{r}{R}\right)^4 + 471582\left(\frac{r}{R}\right)^3 - 392499\left(\frac{r}{R}\right)^2 + 162465\left(\frac{r}{R}\right) - 26738\right]$$

The preferred progression, which is shown in Figure 9 as progression H_8, arises where c_2 = 8.

The design range was denoted in Figure 9 by the limiting curves H_4 where c_2 = 4 as well as H_{10} where c_2 = 10. The line with quadratic symbols depicts the progression of the Λ_{p3} values calculated at discrete locations.

Figure 10 thereby shows the design for a low wind turbine having a tip speed ratio of 9. Again, the design range was shown as in Figure 9, with H_4 for c_2 = 4 and with H_{10} for c_2 = 10. The line with the quadratic symbols depicts the progression of the Λ_{p3} values calculated at discrete locations. Here, the sixth degree polynomial for a continuous progression is as follows:

$$H\left(\frac{r}{R}\right) = c_2 \cdot \Lambda_{p3} = c_2 \cdot \left[\begin{array}{l} 60351.47\left(\frac{r}{R}\right)^6 - 278386.84\left(\frac{r}{R}\right)^5 + -534315.59\left(\frac{r}{R}\right)^4 + 546057.47 \\ \left(\frac{r}{R}\right)^3 - 313179.86\left(\frac{r}{R}\right)^2 + 95422.62\left(\frac{r}{R}\right) - 12015.31 \end{array} \right]$$

The preferred progression, which is illustrated in Figure 10 as H_8, arises where c_2 = 8.

The domain of the polynomial extends over a dimensionless radius $\frac{r}{R}$ = 0.5 to 1.0. In the preferred case, the range falls between $\frac{r}{R}$ = 0.65 to 1.0, however at minimum a range of $\frac{r}{R}$ from 0.7 to 1.0 must be covered.

If a progression of $\frac{r}{R}$ < 0.6 is being considered, there must be an additional calculation of the Λ_{p3} values and the factors of the polynomial members must be adapted.

In so doing, the calculated local Λ_{p3} - value is dependent on the local flow condition at the operating point of the wind power installation being considered. Therefore the final dimension of spike height and distance (or equivalent $\Lambda_{p3}\left(\frac{r}{R}\right)$) must be selected in such a way that the jagged trailing edge is effective at a selected operating point of the wind power installation, optimally the nominal rating.

The calculation of $\Lambda_{p3}\left(\frac{r}{R}\right)$ by means of the Corcos model is not trivial, and can be done more precisely by means of a two-point correlation of wall pressure fluctuation measurements in the wind tunnel near the trailing edge of the profile, as set forth in reference [2].

Figure 11 shows a diagram of the progression of spike heights for one or two embodiments respectively, which heights are scaled for the respective local profile depth over the dimensionless radius for strong wind and low wind design. It can be seen that the design for strong wind has a different characteristic. It is proposed that this be taken into consideration in the design of the spike heights.

Here, Figure 12a, and moreover Figures 12b, 13a and 13b are calculated to scale. It can be seen that the spike height H decreases substantially from a small local radius r_1 to a large local Radius r_2. In order to illustrate this, the spike height H_1 is drawn for the small radius r_1 and the small spike height H_2 is drawn for the large radius r_2. Here, the trailing edge shown is illustrated separately and must still be mounted on a rotor blade for a strong wind turbine. Here, the trailing edge 1 that is shown has a length of approximately 12 meters. It can be seen that the height H_1 is significantly greater than the height H_2 and that the spike height H of the spikes 8 initially remains the same and then drops off sharply at the large, which is to say the outer radius r_2. Due to the simultaneously diminishing profile depth, the relative spike height H of the spikes 8 thus initially increases, namely the spike heights in reference to the respective profile depth, and and then drops off at the end of the rotor blade, namely at r_2.

The illustration in perspective pursuant to Figure 12b again illustrates the progression of the spike height. It can be seen in both figures that along with the spike height, the spike width or the spike distance diminish.

Figures 13a and 13b pertain to a trailing edge 1 for a low wind turbine. It can also be seen that there is a substantial decrease from the spike height H_1 to the spike height H_2, namely from a small radius r_1 to a large radius r_2. The radii r_1 and r_2 of Figure 13a on the one hand, and the Figures 12a and 12b on the other hand, differ from one another in terms of size. At the same time, both trailing edges 1 in Figures 12a and 12b on the one hand, and Figure 13a on the other, are provided for an outer third of the respective rotor blade. In addition, both trailing edges 1 are further divided into segments S_1 to S_5, wherein despite differing trailing edges 1, the same reference signs were used in order to facilitate a comparison. The fifth segment S_5 of the trailing edge 1 of the Figure 13a is also divided into additional sub-segments. In Figure 13a, it can be seen that the spike height H has already decreased in the second segment, whereas a decrease in the second segment of the trailing edge for the strong wind turbine pursuant to Figure 12 is not discernible in the second segment S_2 and does not exist. In that regard, the height progression of the spike height H of the trailing edge 1 for strong wind turbines pursuant to Figures 12a and 12b differs from the progression pursuant to Figure 13a for a low wind turbine.

Figure 13b also shows a section of the trailing edge 1 of the low wind turbine, in order to clarify a possible structural embodiment, in particular of the spikes 8. Accordingly, it can initially be seen that the spikes 8 are connected with one another along a base 30. The spike height H is measured from the base line or base 16, at which the apexes of the recesses 12 are also arranged. Figure 13b also shows that the spike tip 10 may be provided with a slight rounding.

[1] Theory and User Manual BLADOPT, ECN report, August, 2011 by B.H. Bulder, S.A.M. Barhorst, J.G. Schepers, F. Hagg

[2] M. S. Howe. Acoustics of Fluid-Structure Interactions. Cambridge University Press, online ISBN: 9780511662898, hardback ISBN: 9780521633208, paperback ISBN: 9780521054287 edition, 1998.

[3] G. M. Corcos. The structure of the turbulent pressure field in boundary-layer flows. Journal of Fluid Mechanics, 18:353–378, 1964.

[4] Andreas Herrig, Validation and Application of a Hot-Wire based Method for Trailing-Edge Noise Measurements on Airfoils, PhD Thesis, University of Stuttgart, 2011, ISBN 978-3-8439-0578.

From a manufacturing standpoint, the desired progression is preferably created in that a predefined rear lug is machined by means of an automated, computer-controlled cutting process.

Claims

1. A method for constructing a rotor blade of an aerodynamic rotor of a wind power installation, the method comprising the steps of:

determining a trailing edge of the rotor blade, wherein

- the rotor blade has radial positions with respect to the rotor,
- the rotor blade has a local blade profile that is dependent on the radial positions with respect to the rotor,
- the trailing edge has a jagged profile having a plurality of spikes,
- each spike has a spike height and a spike width, and
- at least one of the spike height and the spike width is calculated as a function of the radial position of each spike or as a function of the local blade profile of the radial position of each spike,

wherein the spike height H of the radial positions is calculated from a coherence length scale Λ_{p3} associated with the spike of the radial position, taking into account a constant factor c_2 by using the formula

$$H = c_2 \cdot \Lambda_{p3}.$$

wherein the coherence length scale Λ_{p3} is calculated from a convection velocity U_c and a peak frequency f_{peak}, according to the following calculation:

$$\Lambda_{p3} = \frac{U_c}{\left(2 \cdot \pi \cdot f_{peak}\right)}.$$

wherein the convection velocity U_c is calculated from an effective flow velocity V_{eff} at the blade profile by means of a constant c_1; and

constructing the rotor blade such that the trailing edge has the jagged profile, with the jagged profile comprising the plurality of spikes in accordance with the spike height H, as determined based on the radial position of each spike of the plurality of spikes.

2. The method according to Claim 1,
characterized in that
the spike height is greater than the spike width, the spike width is calculated from the spike height and therefore the ratio of the spike height to the spike width falls in the range of 0.5 to 10.

3. The method according to Claim 1 or 2,
characterized in that
at least one of the spike height and the spike width depends on the local radius of each spike by means of a fourth to eighth degree polynomial relationship.

4. The method according to any one of Claims 1 to 3,
characterized in that
the spikes have at least one of spike widths and spike heights that vary in relation to one another.

5. The method according to any one of Claims 1 to 4,
characterized in that
the calculation comprises setting up the rear edge in such a way that, in the case of trailing edges for low-wind locations, the spike height of the spikes has a greater decrease in the spikes as a radius of the radial position of the spikes increases than in the case of trailing edges for strong-wind locations, or that the spike height of the same radial position in the case of trailing edges for wind power installations for low-wind locations is lower than in the case of trailing edges for wind power installations in strong-wind locations of a same power class.

6. A method for constructing a rotor blade of an aerodynamic rotor of a wind power installation, the method comprising the steps of:

determining a rear edge of the rotor blade, wherein

- the rotor blade has radial positions with respect to the rotor,
- the rotor blade has a local blade profile that is dependent on the radial positions with respect to the rotor,
- the rear edge has a jagged profile having a plurality of spikes,
- each spike has a spike height and a spike width, and
- at least one of the spike height and the spike width is calculated as a function of the radial position of each spike or as a function of the local blade profile of the radial position of each spike,

wherein the calculation of the spike height H of the radial position, is calculated from an associated flow velocity V_{eff}, an associated peak frequency f_{peak} of the noise spectrum and a predetermined factor k using the formula

$$H = k \cdot \frac{V_{eff}}{f_{peak}};$$

constructing the rotor blade such that the rear edge has the jagged profile, with the jagged profile comprising the plurality of spikes in accordance with the spike height H, as determined based on the radial position of each spike of the plurality of spikes.

7. A rotor blade for a wind power installation, comprising
a longitudinal axis,
a rear edge, and
a local blade profile that is dependent on positions along the longitudinal axis,

wherein the rear edge has a jagged profile having a plurality of spikes,

wherein each spike has a spike height and a spike width,

wherein at least one of the spike height and the spike width is a function of the position of the spike along the longitudinal axis or is a function of the local blade profile of the position along the longitudinal axis,

wherein the spike height H of the radial positions is calculated from a coherence length scale Λ_{p3} associated with the spike of the radial position, taking into account a constant factor c_2 by using the formula

$$H = c_2 \cdot \Lambda_{p3}.$$

wherein the coherence length scale Λ_{p3} is calculated from a convection velocity U_c and a peak frequency f_{peak}, according to the following calculation:

$$\Lambda_{p3} = \frac{U_c}{\left(2 \cdot \pi \cdot f_{peak}\right)}.$$

wherein the convection U_c is calculated from an effective flow velocity V_{eff} at the blade profile by means of a constant c_1.

8. A rotor blade for a wind power installation, comprising
a longitudinal axis,
a rear edge for a rotor blade of an aerodynamic rotor of a wind power installation,
a local blade profile that is dependent on positions along the longitudinal axis,

wherein the rear edge has a jagged profile having a plurality of spikes,

- wherein each spike has a spike height and a spike width,
- wherein at least one of the spike height and the spike width is a function of the position of the spike along the longitudinal axis or is a function of the local blade profile of the position along the longitudinal axis,
- wherein the calculation of the spike height H of the radial position is calculated from an associated flow velocity V_{eff}, an associated peak frequency f_{peak} of the noise spectrum and a predetermined factor k using the formula

$$H = k \cdot \frac{V_{eff}}{f_{peak}}.$$

9. The rotor blade for a wind power installation according to Claim 8, characterized in that
the spike height is greater than the spike width and the ratio of the spike height to the spike width falls in the range of 0.5 to 10.

10. The rotor blade for a wind power installation according to Claim 8 or 9, characterized in that
at least the spike height and the spike width depends on the position of the spike by means of a fourth to eighth degree polynomial function.

11. A wind power installation having a rotor blade pursuant to Claim 7 or 8.

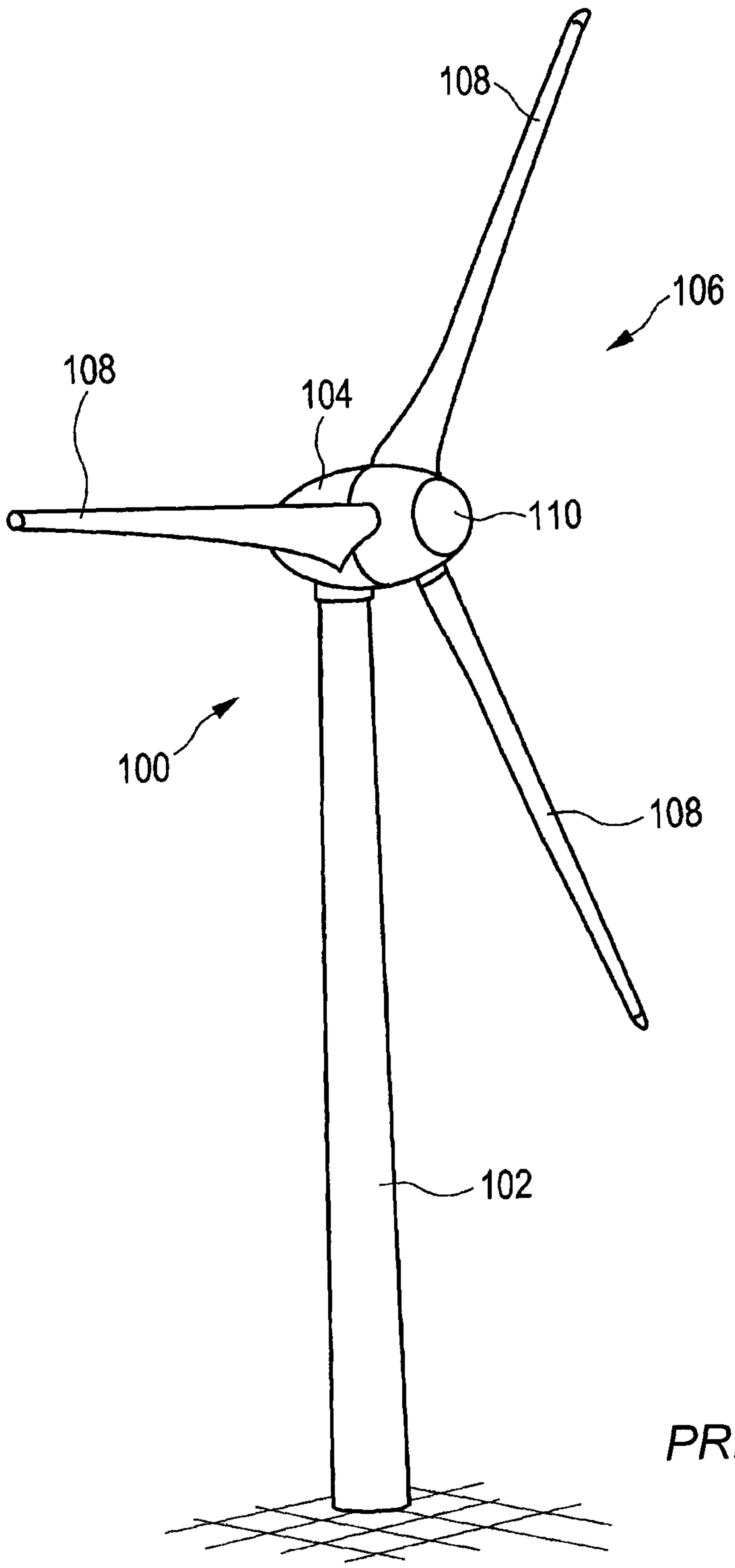

PRIOR ART

Fig. 1

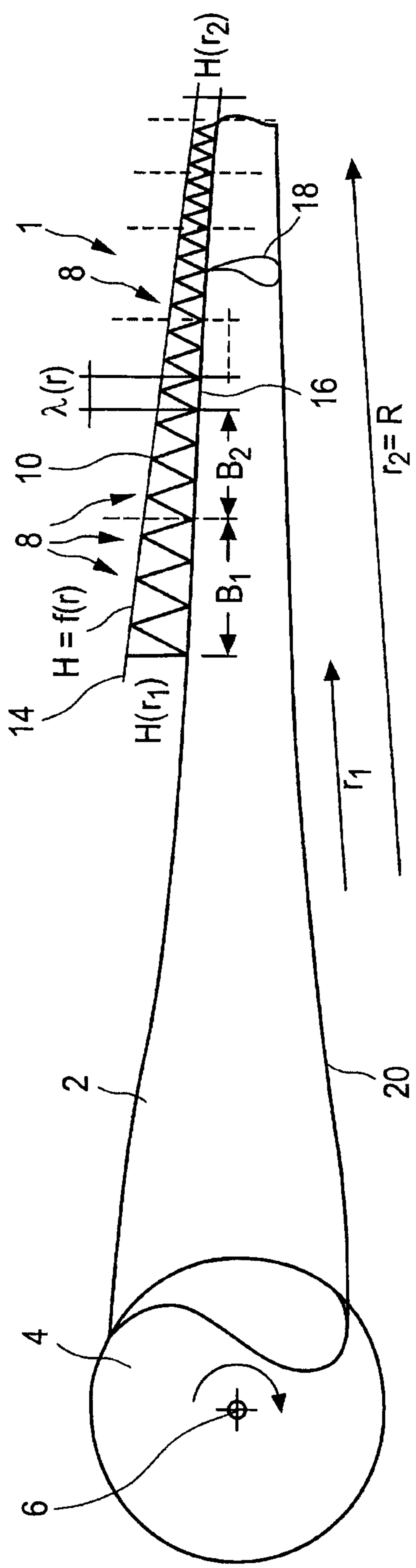

Fig. 2

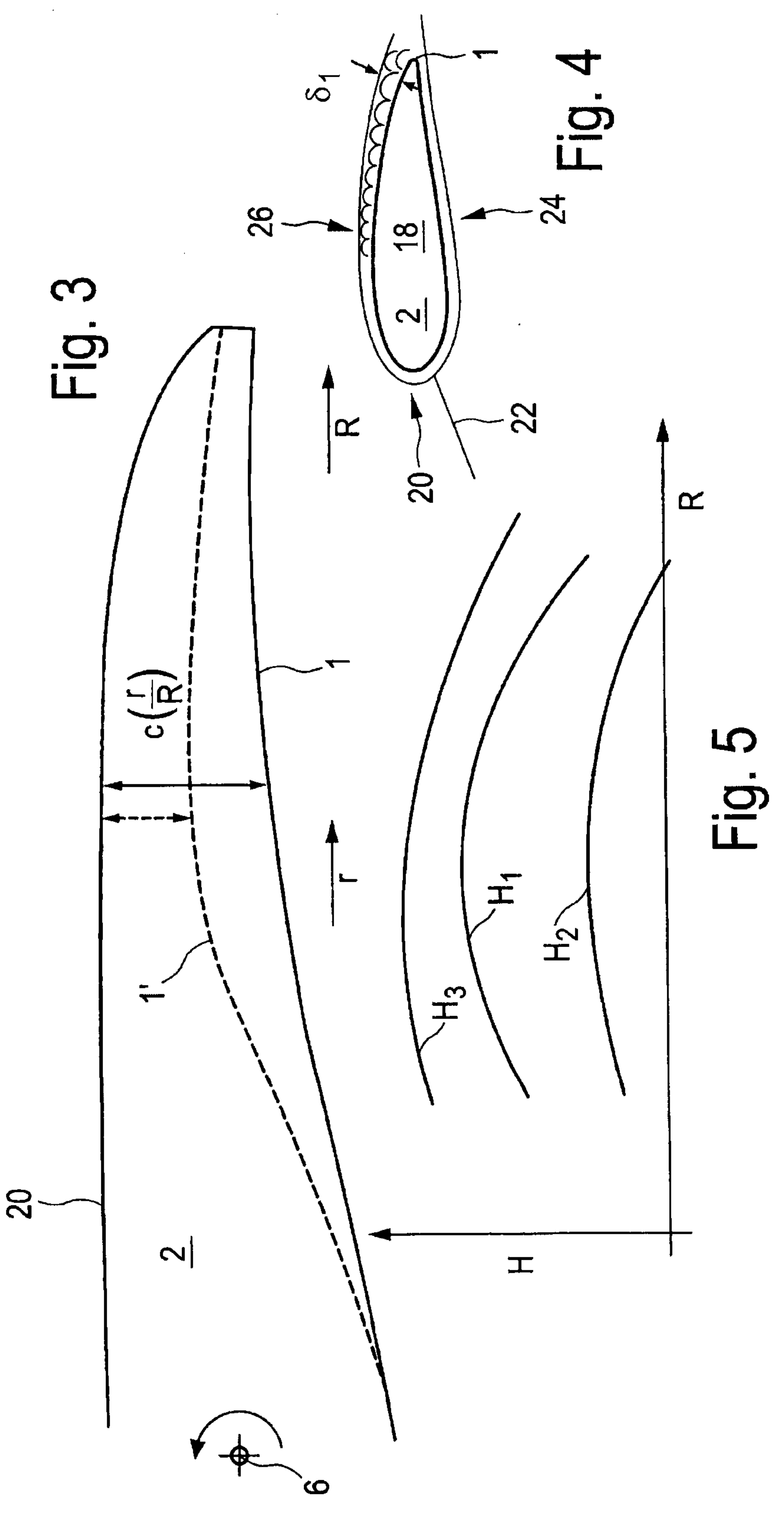

Fig. 3

Fig. 4

Fig. 5

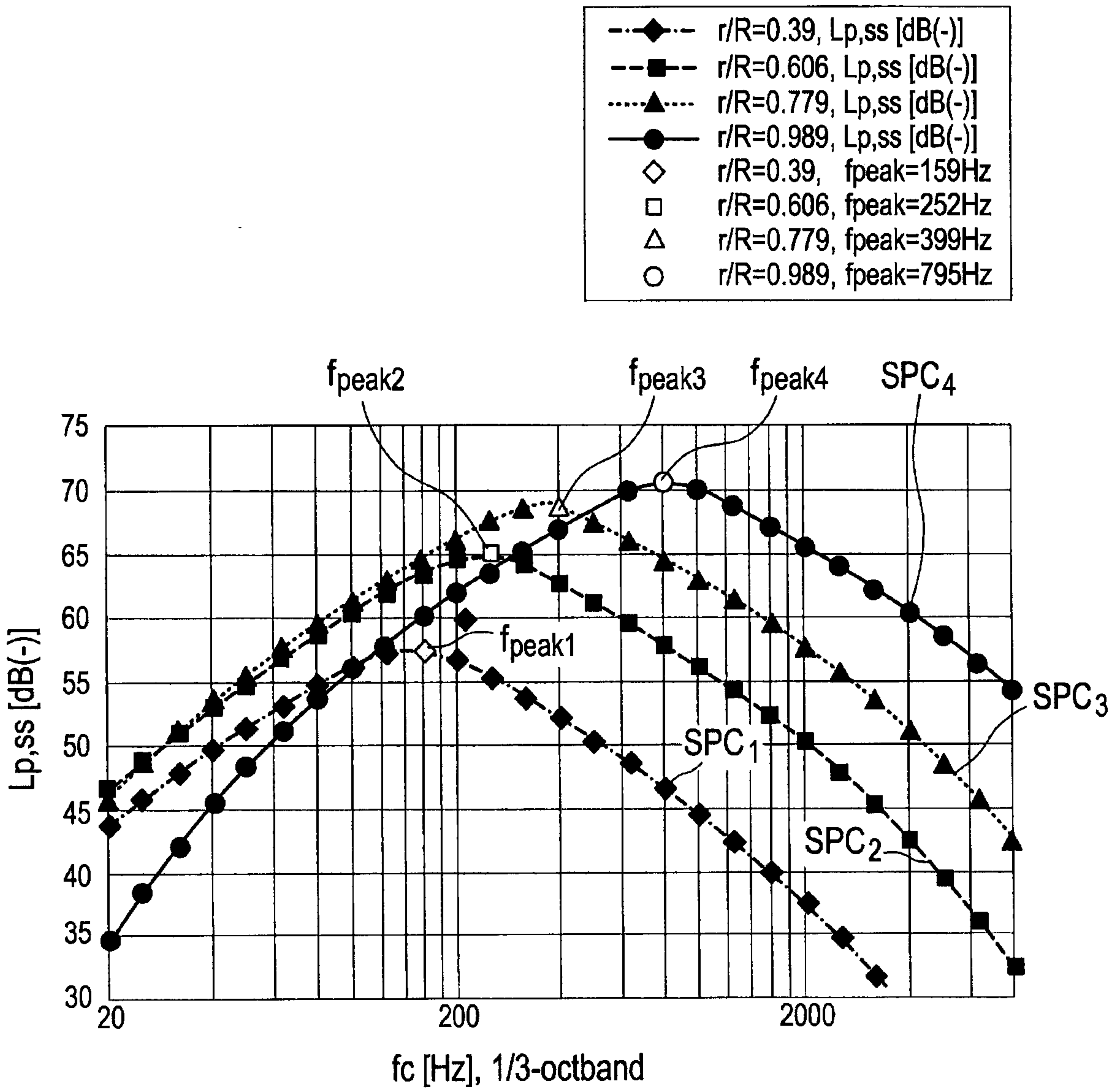
r/R=0.39, Lp,ss [dB(-)]
r/R=0.606, Lp,ss [dB(-)]
r/R=0.779, Lp,ss [dB(-)]
r/R=0.989, Lp,ss [dB(-)]
r/R=0.39, fpeak=159Hz
r/R=0.606, fpeak=252Hz
r/R=0.779, fpeak=399Hz
r/R=0.989, fpeak=795Hz
fpeak2
fpeak3
fpeak4
SPC4
fpeak1
SPC3
SPC1
SPC2
75
70
65
60
55
50
45
40
35
30
20
200
2000
Lp,ss [dB(-)]
fc [Hz], 1/3-octband

Fig. 6

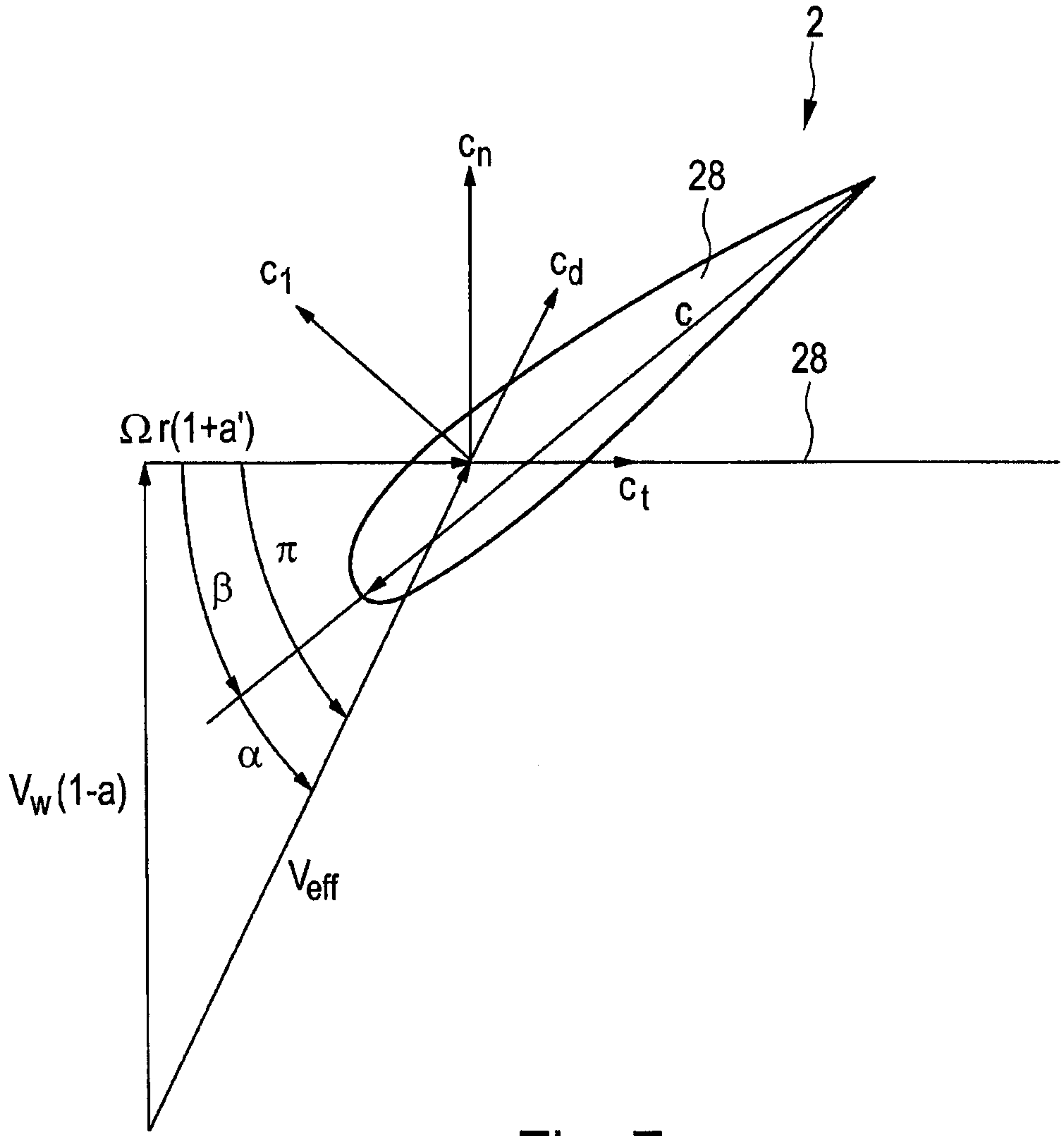

Fig. 7

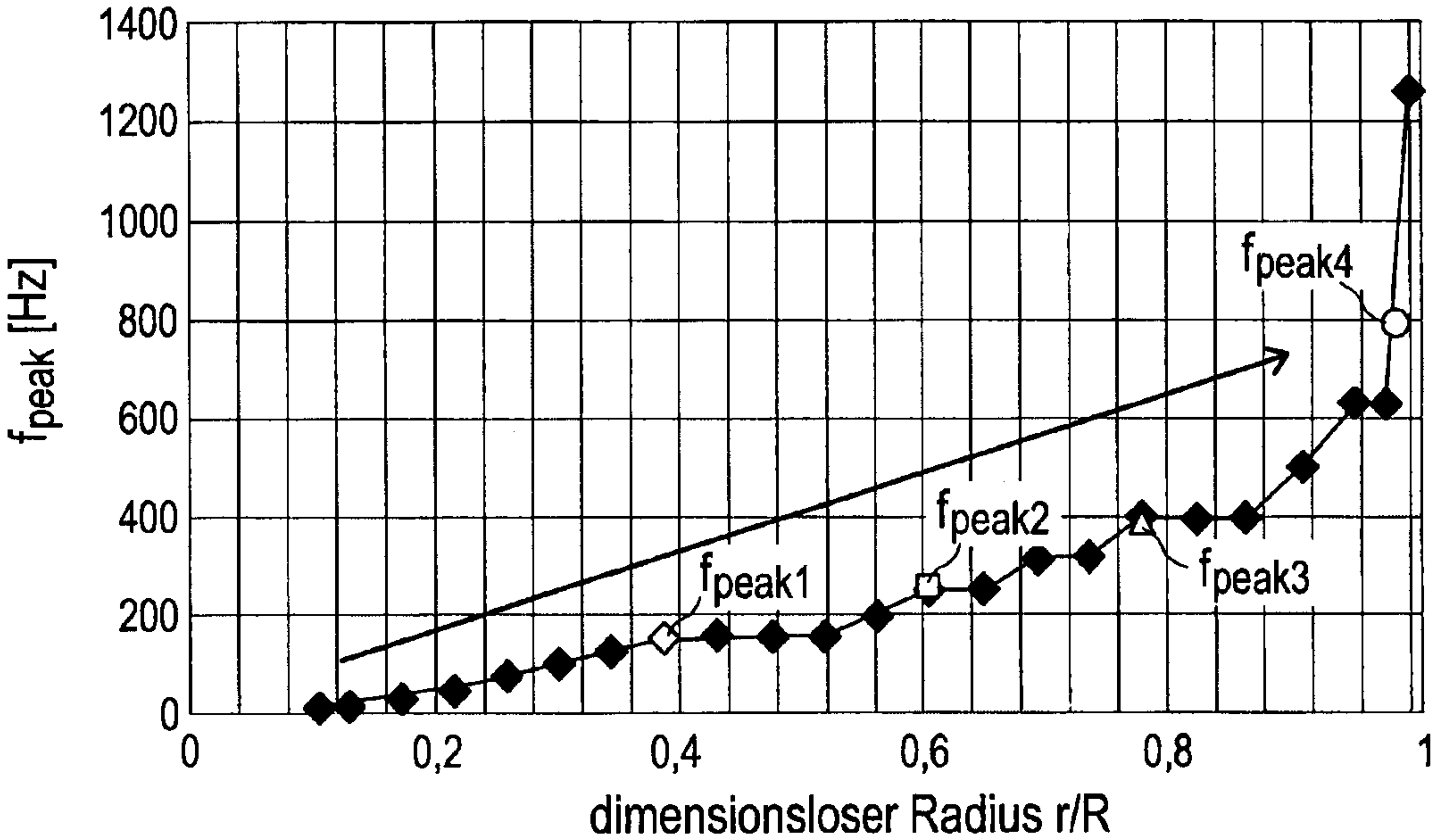

1400
1200
1000
800
600
400
200
0
fpeak [Hz]
0
0,2
0,4
0,6
0,8
1
dimensionsloser Radius r/R
fpeak1
fpeak2
fpeak3
fpeak4

Fig. 8

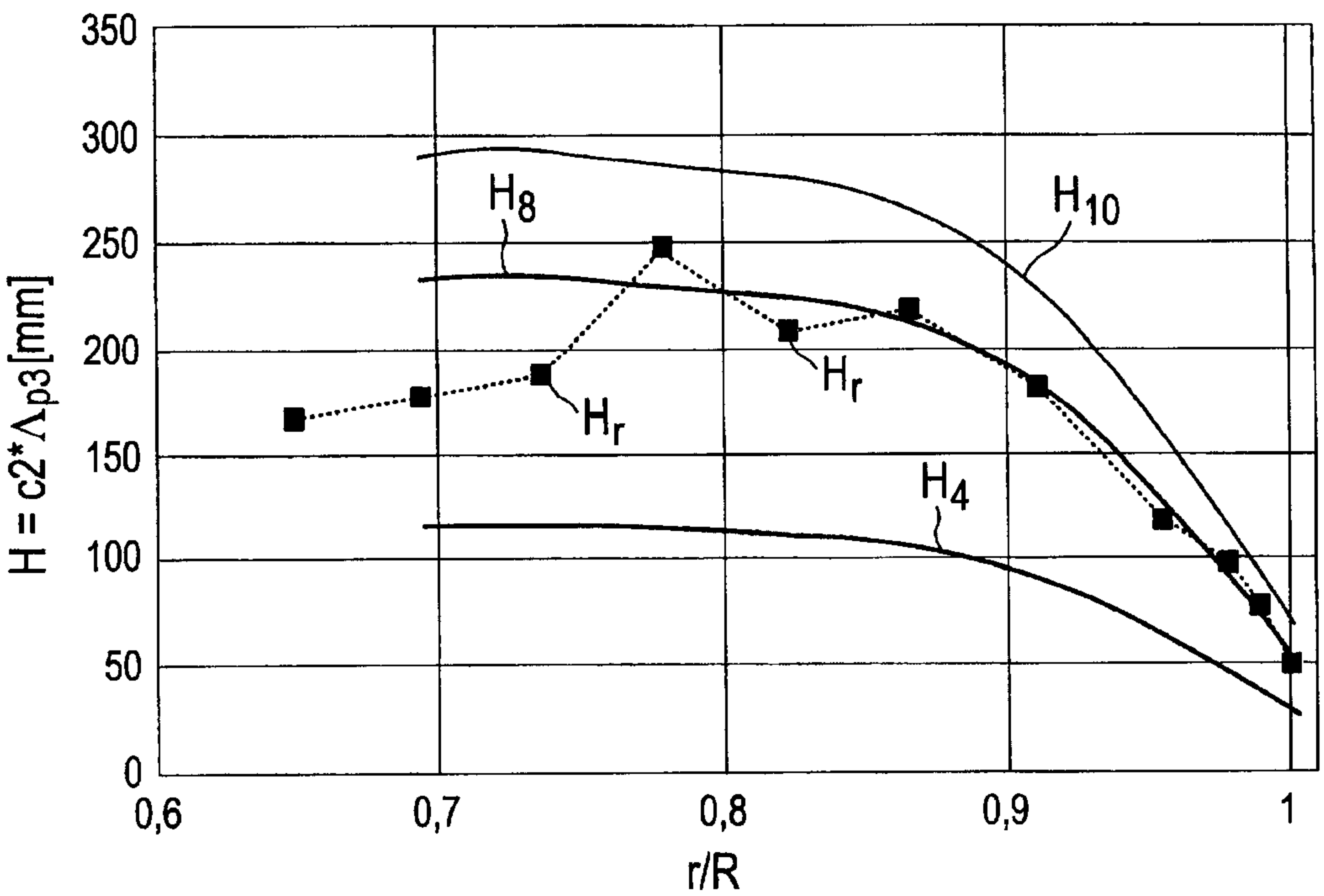

350
300
250
200
150
100
50
0
H = c2*Λp3[mm]
0,6
0,7
0,8
0,9
1
r/R
H8
H10
Hr
Hr
H4

Fig. 9

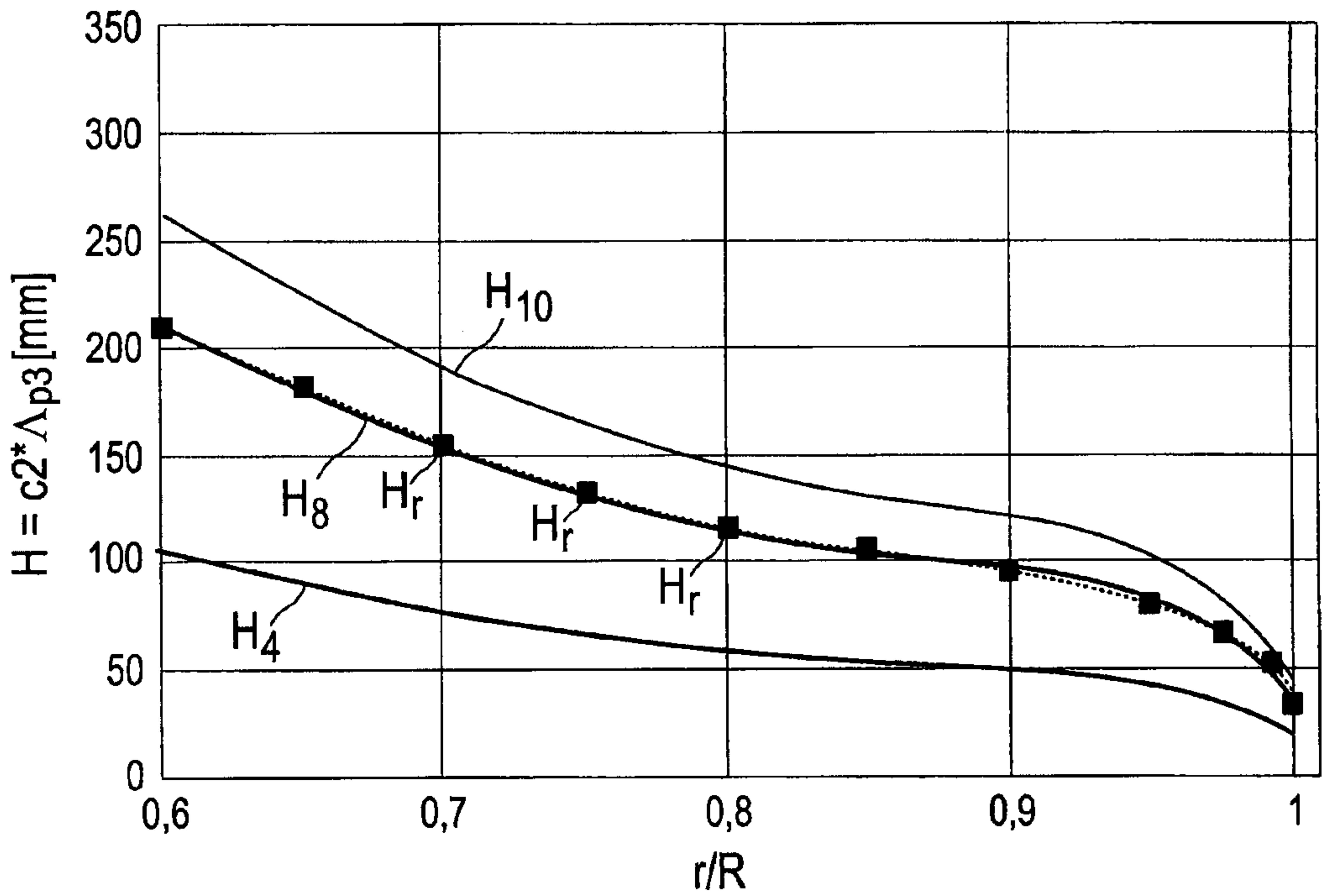
350
300
250
200
150
100
50
0
H = c2*Λp3 [mm]
H10
H8
Hr
Hr
Hr
H4
0,6
0,7
0,8
0,9
1
r/R

Fig. 10

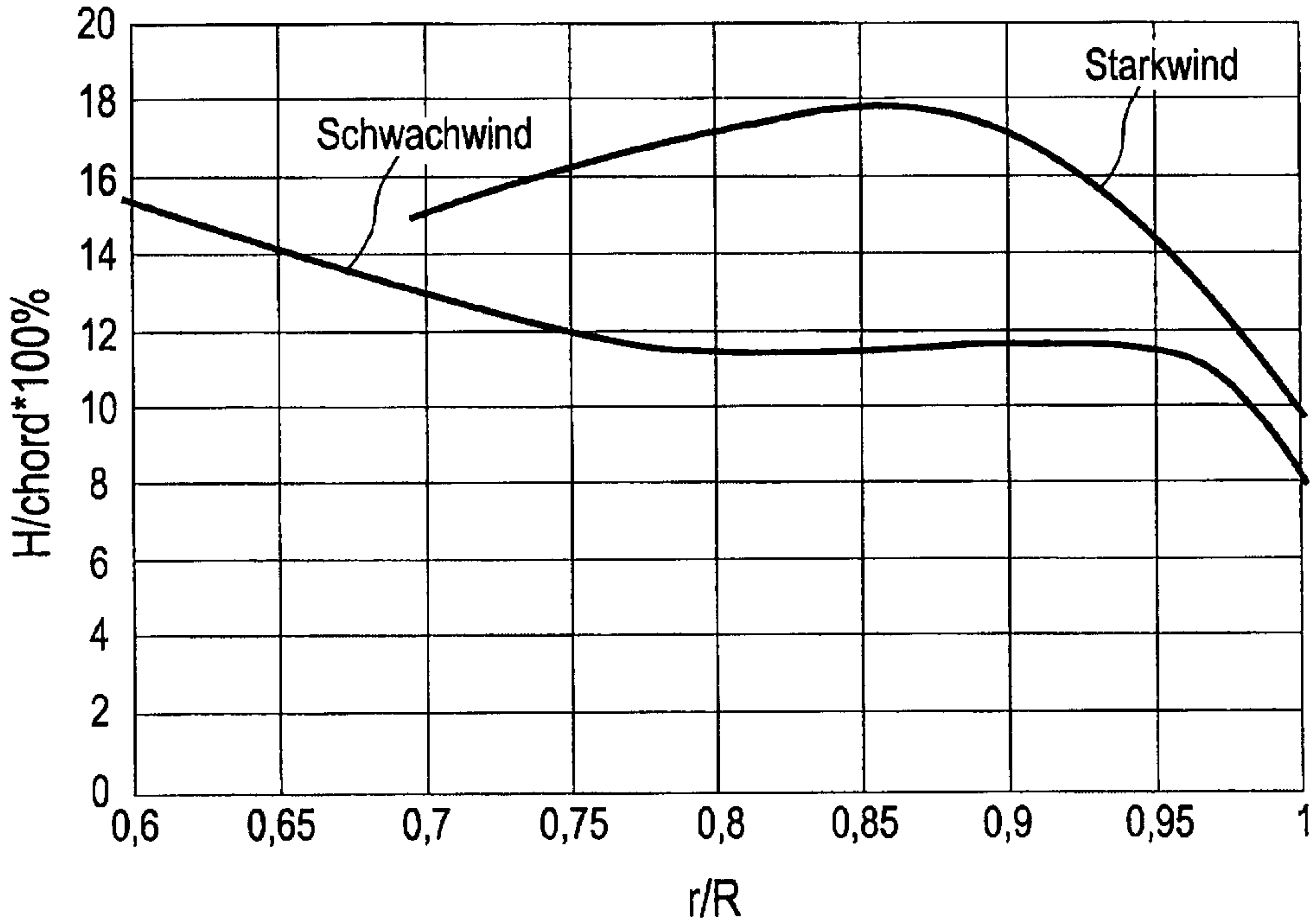

20
18
16
14
12
10
8
6
4
2
0
H/chord*100%
Schwachwind
Starkwind
0,6
0,65
0,7
0,75
0,8
0,85
0,9
0,95
1
r/R

Fig. 11

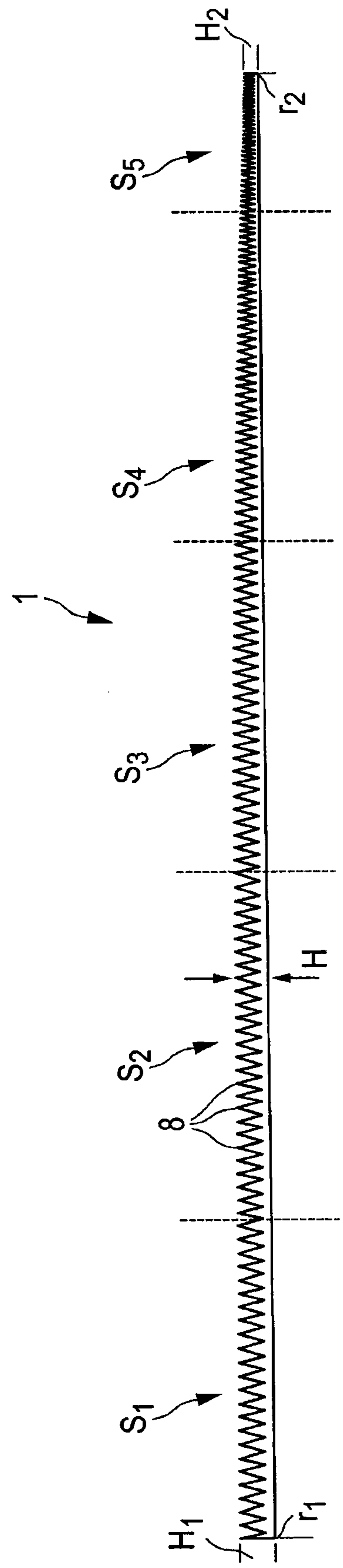

Fig. 12a

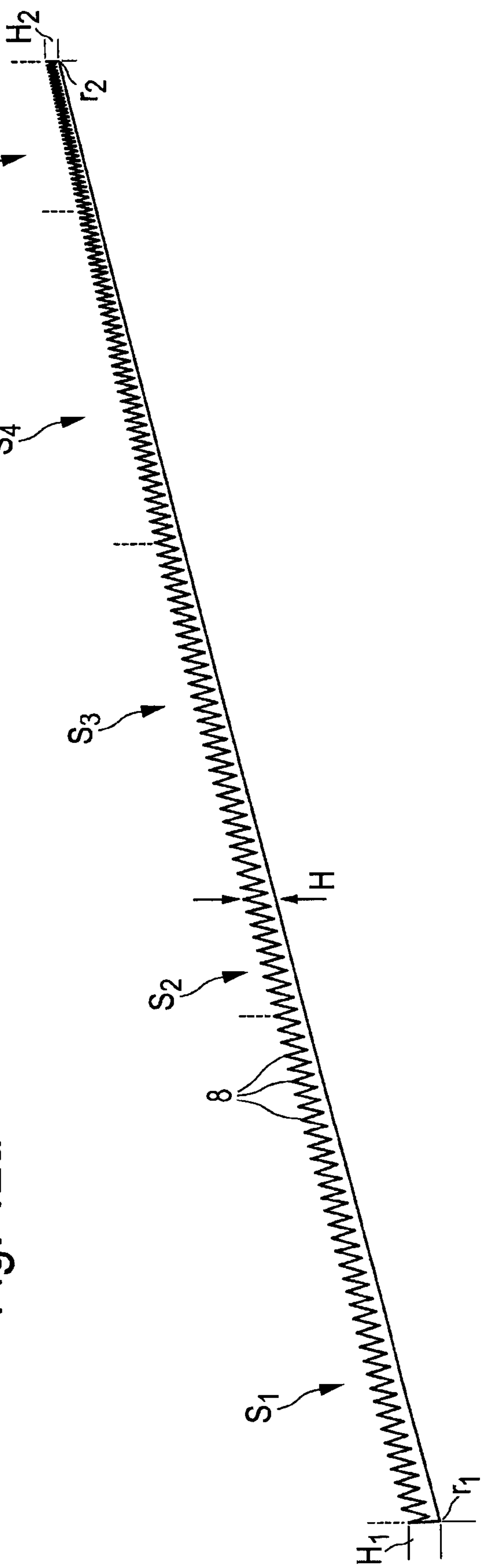

Fig. 12b

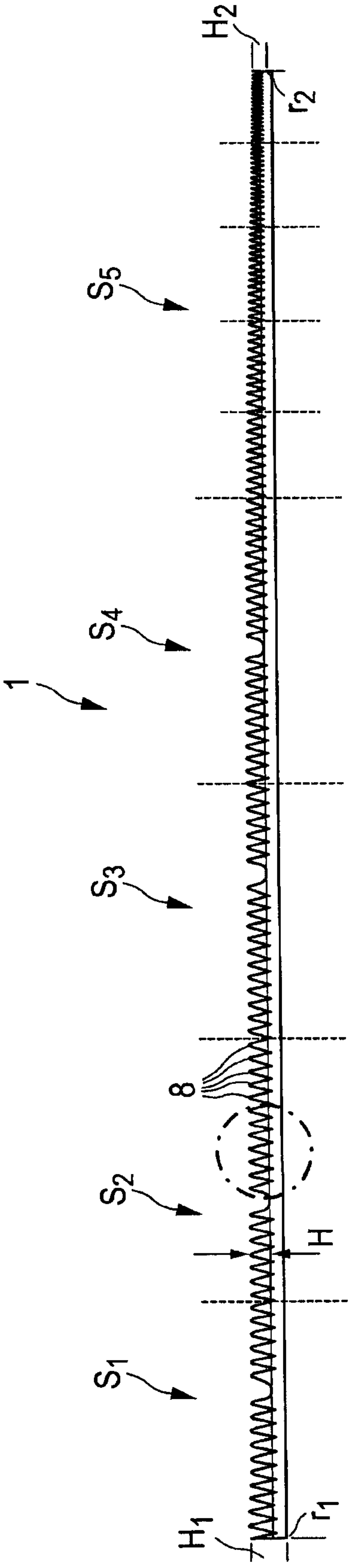

Fig. 13a

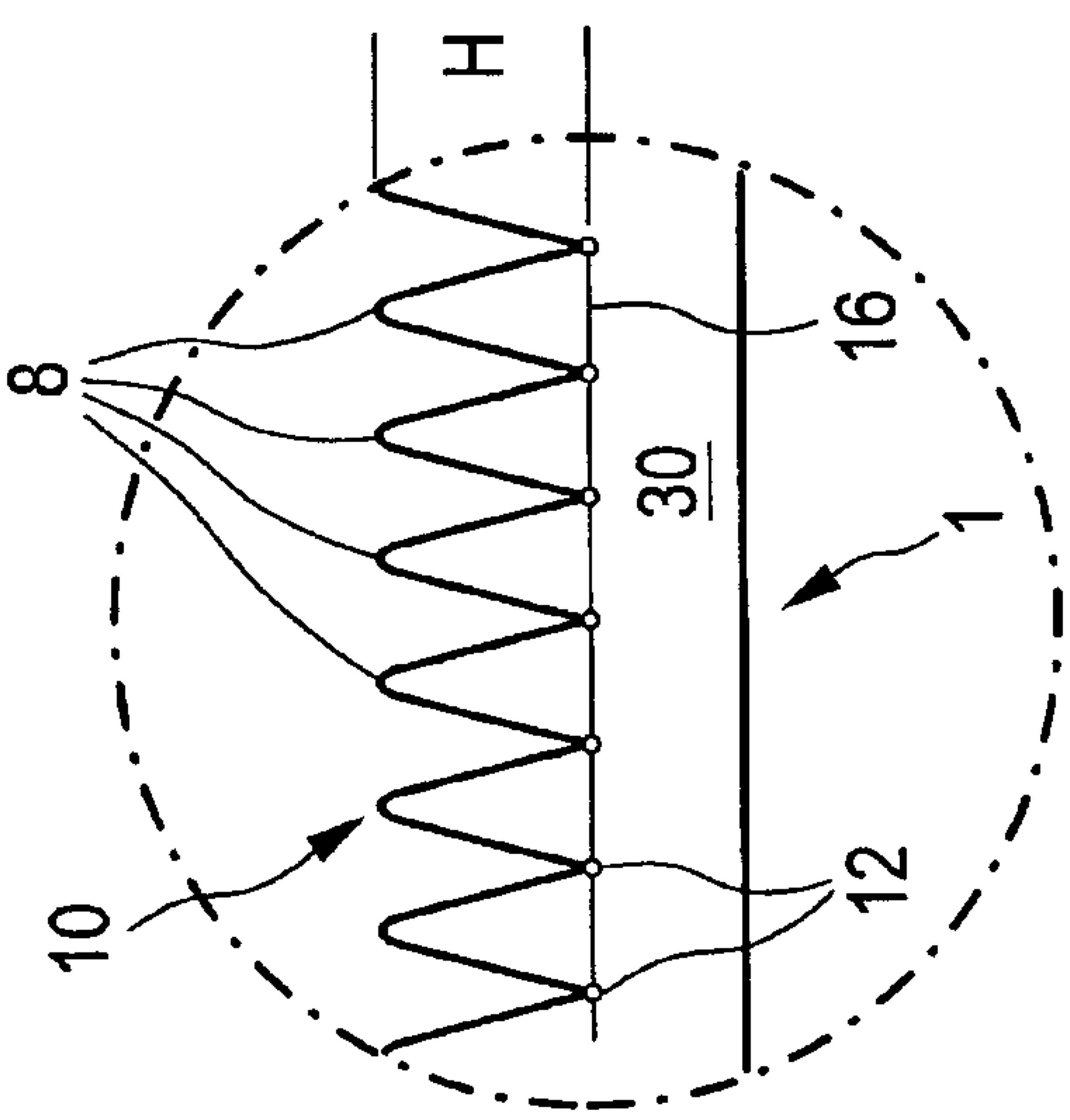

Fig. 13b

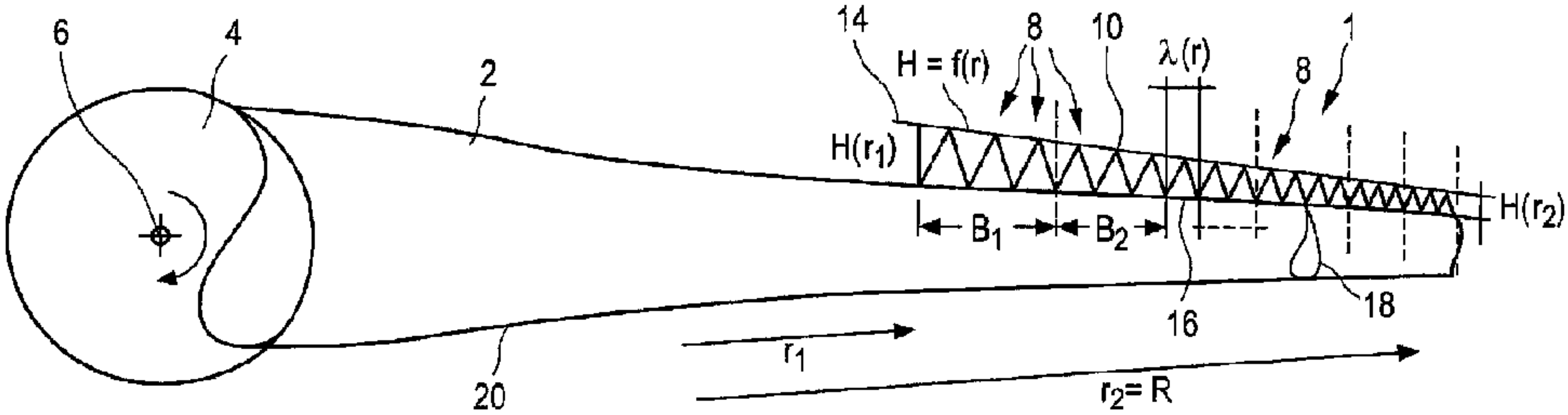
6
4
2
14
H = f(r)
8
10
λ(r)
1
8
8
H(r1)
H(r2)
B1
B2
16
18
20
r1
r2= R